2-D Array Photonic Crystal Sensing Motif

Jian-Tao Zhang, Luling Wang, Jia Luo, Alexander Tikhonov, Nikolay Kornienko, and Sanford A. Asher*

Department of Chemistry, University of Pittsburgh, Pittsburgh, Pennsylvania 15260, United States

S *Supporting Information*

ABSTRACT: We have developed the first high-diffraction-efficiency two-dimensional (2-D) photonic crystals for molecular recognition and chemical sensing applications. We prepared close-packed 2-D polystyrene particle arrays by self-assembly of spreading particle monolayers on mercury surfaces. The 2-D particle arrays amazingly diffract 80% of the incident light. When a 2-D array was transferred onto a hydrogel thin film showing a hydrogel volume change in response to a specific analyte, the array spacing was altered, shifting the 2-D array diffraction wavelength. These 2-D array photonic crystals exhibit ultrahigh diffraction efficiencies that enable them to be used for visual determination of analyte concentrations.

It is essential to identify and quantitate hazardous chemical or biological agents remotely before they achieve dangerous levels. The ideal sensing technology would be able to separately and selectively detect the largest subset of chemical and biological agents with high sensitivity. This has motivated the development of numerous sensing approaches.[1] Many of these approaches rely on sophisticated analytical techniques such as mass spectrometry, fluorescence, Raman, etc.,[2] that have disadvantages of complexity and high cost.

Attractive approaches to chemical sensing would use methods that require no sample preparation and allow the visual determination of the chemical species and their concentrations.[3] In one example of such an approach, we previously developed 3-D polymerized colloidal crystal array (PCCA) hydrogel sensing materials, where the analyte concentration was determined from the PCCA diffraction.[4a−c] These 3-D photonic crystal materials were fabricated by self-assembly of face-centered cubic (fcc) arrays of colloidal particles followed by a polymerization that embedded the colloidal crystal array (CCA) within a hydrogel network.[4] The PCCA was then functionalized with the appropriate molecular recognition agents. These sensing materials were developed to detect analytes such as creatinine, glucose, pH, organophosphorus compounds, amino acids, metal ions, etc.[4a−c] In a similar approach, Li and co-workers[3a] reported the use of inverse 3-D ordered photonic materials to detect anions.

Here we describe a new sensing motif that utilizes 2-D monolayer arrays of particles attached to molecular recognition polymer hydrogel networks. The visually evident diffraction color of the 2-D array is altered because the hydrogel network swells or shrinks in response to analyte concentration changes.

Recently, a number of groups have fabricated 2-D arrays for chemical sensing applications. In all previous cases, the chemical
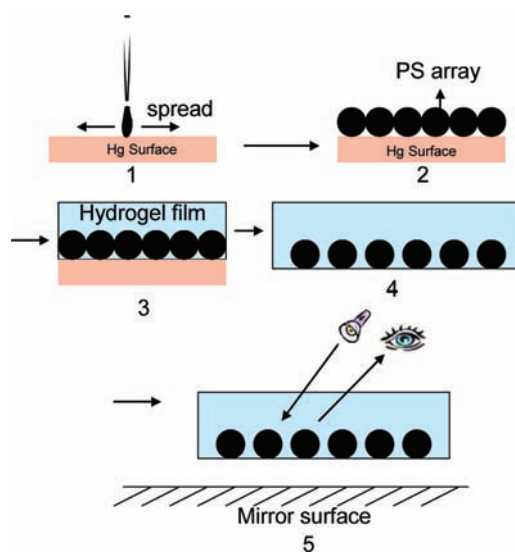

Figure 1. Fabrication of a 2-D photonic crystal for sensing applications. (1) A water/propanol PS particle dispersion is dropped onto a Hg surface. (2) The dispersion spreads to form a 2-D close-packed PS particle array as the solvent evaporates. (3) A hydrogel film is polymerized around the 2-D array. (4) The swelled hydrogel with the embedded 2-D array is peeled from the glass substrate. (5) Diffraction from the 2-D array/hydrogel sandwich is monitored visually.

sensitivity relied on refractive index changes that shift plasmon resonances or the frequency of a defect mode within the band gap to monitor the analyte.[5] In contrast, our approach is intrinsically more sensitive because we utilize hydrogel volume changes that give rise to very large changes in the 2-D array diffraction wavelength. In addition, by using a mirror substrate, we generate very intense diffraction from the 2-D array monolayer, allowing it to be easily monitored visually.

Figure 1 illustrates the fabrication of a 2-D CCA attached to a hydrogel. We first prepared a well-ordered 2-D close-packed array of 580 nm diameter polystyrene (PS) spheres on a Hg surface. This was accomplished by placing a drop of a 13.3% (w/v) dispersion of PS particles in aqueous propanol onto a Hg surface. Because liquids with moderate surface tension spread readily on Hg as thin films, the colloidal particle suspension spread rapidly, during which the 2-D PS particle monolayer self-assembled as the solvent evaporated.[6]

Figure 2a shows that the self-assembled ordered 2-D monolayer brightly diffracts over 80% of the incident light back toward the observer. Figure 2b shows an SEM image demonstrating high
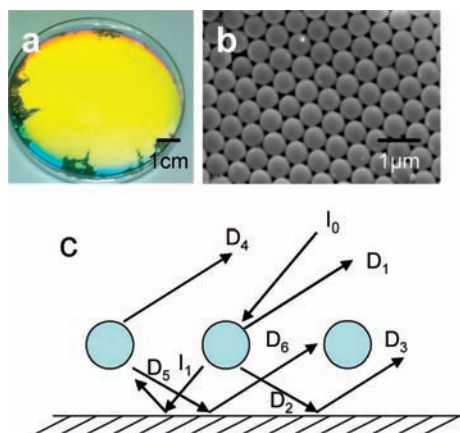
Figure 2. (a) Photograph showing bright diffraction of yellow light from a PS particle array on a Hg surface. The array was illuminated by white light at an incident angle of 27° and observed at 45° from the normal. (b) SEM images of a 2-D PS array transferred onto a plastic sheet after sputter coating of Au. (c) Proposed mechanism giving rise to the strong diffraction. In the case of Hg, there was no gap between the 2-D array and the Hg surface. In contrast, in some experiments on mirrors, there was a gap that was filled by air, glass, or a plastic spacer.

Figure 3. Diffraction by 2-D arrays on different mirror surfaces: (a) Hg; (b) Au; (c) glass-surface mirror; (d) plastic film. The measurement angle between the probe and the normal to the 2-D array was 38°. The large beam divergence of the excitation fiber and the large acceptance angle of the collection fiber broadened the diffraction bandwidth.

ordering of the hexagonal 2-D array of PS spheres formed by self-assembly on the Hg surface with a domain size of ~10 μm (see Figure S1 in the Supporting Information). We believe that the present work is the first to observe high-efficiency 2-D diffraction from 2-D arrays on Hg surfaces. The very bright diffraction results from the combined diffraction of four beams (Figure 2c). The 2-D array diffracts the incident light (I_0) back toward the observer on the incident side, giving rise to a rather weak diffracted beam (D_1). The more intense 2-D array forward-diffracted beam (D_2) is back-reflected to the observer by the Hg surface, forming an intense beam (D_3) that propagates parallel to D_1.[8] In addition, the remaining incident light (I_1) is transmitted (i.e., zeroth-order-diffracted) through the 2-D array and back-reflected by the Hg surface. This beam is forward-diffracted by the 2-D array to form the diffracted incident beam (D_4), which also propagates parallel to D_1. The back-diffracted beam D_5 is reflected to form beam D_6, which also propagates parallel to D_1. The total intensity of diffracted light is the sum of the intensities of beams D_1, D_3, D_4, and D_6, which is comparable to that of the incident light. We will soon present a detailed mechanism that quantitatively explains this high diffraction efficiency.[8]

We probed the diffraction using a six-around-one reflection probe that produces excitation with white light from a central fiber and collects the back-diffracted light with a closely surrounding set of six fibers in a Littrow configuration. Figure 3 compares the diffracted intensity of a PS 2-D array on a transparent plastic film to the diffracted intensity of this same film placed on Hg and other mirror surfaces. The diffracted intensity from the 2-D array on the Hg surface was 15-fold larger than that from the 2-D array on the plastic film, indicating the strong reflection enhancement. Other flat reflective surfaces also increased the diffracted intensity. For example, a front-surface gold mirror and a glass-surface mirror increased the diffraction efficiency 6- and 2.7-fold relative to the plastic film (Figure 3). The resulting very bright back-reflection makes it easy to monitor the 2-D array diffraction visually or instrumentally.
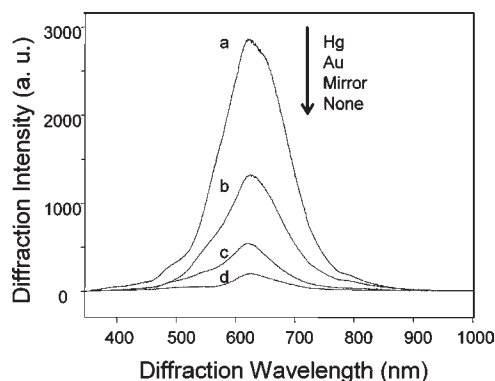
For most sensing applications, it would be preferable to utilize a non-close-packed array, which would allow the particle spacing to swell or shrink when attached to a hydrogel that is responsive to specific analyte concentrations. We fabricated a non-close-packed sensing array by transferring the 2-D array onto a hydrogel that contains molecular recognition agents (Figure 1). The molecular recognition agents are designed to cause reversible hydrogel swelling/shrinking due to analyte-induced alterations in the hydrogel osmotic pressure, resulting in changes in the 2-D lattice spacing that cause shifts in the diffracted wavelength.

We transferred the 2-D array onto a thin hydrogel layer attached to a glass slide by layering a polymerization solution [a 1 mL aqueous solution containing 10 wt % acrylamide (AAm), 0.2 wt % N,N-methylenebis(acrylamide) (MBAAm), 20 μL of acrylic acid (AAc), and 10 μL of Irgacure 2959 (33% (w/v) in DMSO)] onto the 2-D array. A glass slide (60 mm × 24 mm × 0.12 mm) was placed on the polymerization solution on top of the 2-D array. This slide displaced excess polymerization solution from the top of the 2-D array.

Polymerization was initiated by UV light from a Blak Ray lamp (365 nm, 5–10 min). The resulting hydrogel-film-embedded 2-D array was removed from the Hg surface by lifting the glass slide and then peeled from the glass slide and rinsed with large amounts of water. Alternatively, a crown ether-containing hydrogel-film-embedded 2-D array was fabricated by replacing the AAc with 30 μL of a 1:2 (w/v) solution of 4-acryloylamidobenzo-18-crown-6 (4AB18C6) in DMSO .

Figure 4a shows an SEM image of the air-dried 2-D array on the poly(acrylamide-co-acrylic acid) (PAAm–AAc) hydrogel on the glass slide. Figure 4b shows that the polymerized hydrogel was localized at the glass interface with the PS particle array protruding from the hydrogel. Analysis of the SEM image in Figure 4d indicated that the 2-D ordering was not significantly degraded by the polymerization and transfer process.

Placing this 2-D-array-containing hydrophilic hydrogel in water swelled the hydrogel and increased the 2-D array spacing, which produced a red shift in the diffraction (Figure 4c); within 10 min, the diffraction was red-shifted from 621 to 653 nm, and it reached equilibrium at 664 nm in less than 30 min. Figure 4d shows an SEM image of the PS particle array on the PAAm–AAc hydrogel that had previously been swollen in water. A heavy metal washer placed on the swollen 2-D-array-containing
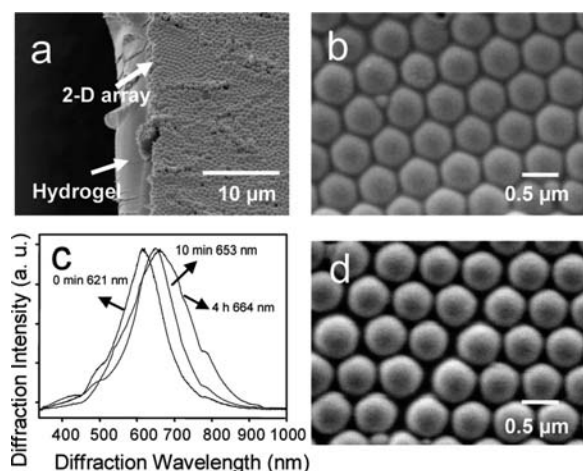
Figure 4. (a) SEM image of a PS array on a PAAm−AAc hydrogel film at a tilt angle of 20°. (b) High-resolution SEM image of the 2-D PS array on the PAAm-AAc hydrogel. (c) Back-diffraction by close-packed 2-D arrays on a PAAm−AAc hydrogel swollen in water for 0 min, 10 min, and 4 h. The measurement angle between the probe and the normal to the 2-D array was 38°. We measured the diffraction with the array on top of a gold mirror. (d) High-resolution SEM image of the non-close-packed PS particles on the swollen PAAm−AAc hydrogel. SEM was used to monitor the section of the 2-D array film dried in air. The spacing between particle surfaces was calculated to be 42 nm.

hydrogel film prevented the central area from shrinking on drying. This maintained the hydrated 2-D particle array spacing.

In the Littrow configuration, the 2-D Bragg diffraction relationship is $m\lambda = 3^{1/2}d \sin \theta$, where m is the diffraction order, λ is the diffracted wavelength (in vacuum), d is the 2-D particle spacing, and θ is the angle of the light relative to the normal to the 2-D array. The 2-D diffracted wavelength is independent of the refractive index.[7] The diffraction studied here resulted from the shortest 2-D reciprocal lattice vector. Thus, for a defined θ, λ was proportional to the spacing between particles. From our experimental data, we calculated that $\lambda_{dried}/d_{dried} = (621 \text{ nm})/(580 \text{ nm}) = 1.072$, which is quite close to the value $\lambda_{swollen}/d_{swollen} = (662 \text{ nm})/(622 \text{ nm}) = 1.064$, demonstrating that the diffraction wavelength varied with the particle spacing.

We copolymerized AAc into the hydrogel to fabricate a pH-responsive material. Figure 5a shows the pH dependence of the diffraction from this 2-D array in a buffer solution containing 150 mM NaCl. As shown in Figure 5a, the diffraction was red-shifted from 620 to 668 nm between pH 3.22 and 7.91 as the AAc carboxyl groups became ionized. The change in color was clearly and visually evident. Carboxyl group ionization immobilized counterions within the hydrogel, resulting in an osmotic pressure due to the increased Donnan potential that swelled the hydrogel, as observed earlier for 3-D photonic crystals.[9] These pH diffraction shifts were fully reversible over multiple pH cycles.

We also fabricated a 2-D sensing material for monitoring of Pb^{2+} by copolymerizing 4AB18C6 into the hydrogel. This crown ether selectively complexes Pb^{2+} to immobilize charge onto the hydrogel, which also results in an increased osmotic pressure due to the Donnan potential arising from the mobile counterions, just as in the pH sensor.[9,10] The Pb^{2+} binding forms a polyelectrolyte hydrogel whose charge state is determined only by the number of bound Pb^{2+} ions. The swelling of the hydrogel increases with
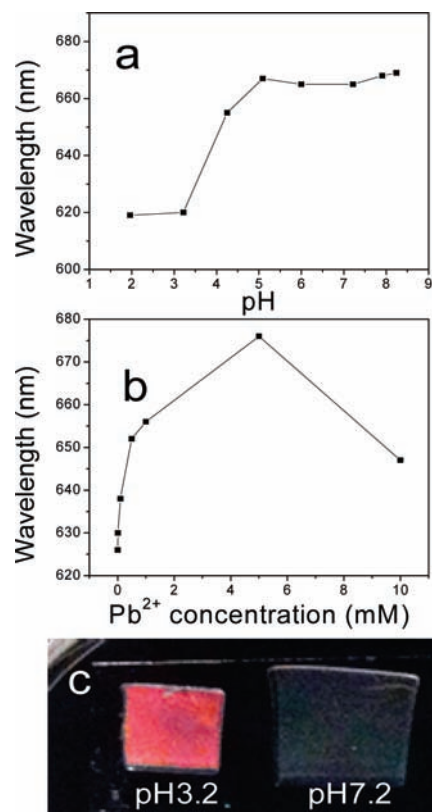

Figure 5. (a) pH dependence of the diffraction wavelength of the 2-D array/PAAm−AAc hydrogel sensors after equilibration in pH buffer solutions containing 150 mM NaCl. (b) Pb^{2+} dependence of the diffraction wavelength of 2-D array/PAAm−4AB18C6 hydrogel sensors after equilibration at different concentrations of Pb^{2+} in water. The measurement angle between the probe and the normal to the 2-D array was 38°; all diffraction measurements were obtained from the 2-D array/hydrogel on top of a gold mirror. (c) Optical photograph taken close to the Littrow configuration at an angle of ∼38° to the 2-D array normal, showing the 2-D PS array/hydrogel-diffracted colors at pH 3.2 and 7.2. The 2-D array/hydrogel samples were placed on a Hg surface. At pH 7.2, the diffraction was in the near-IR and thus invisible, leaving the image dark.

the number of attached charged groups. Figure 5b shows the dependence of the diffraction wavelength on the Pb^{2+} concentration. Below 5 mM, the diffraction was red-shifted with increasing Pb^{2+} concentration, while above 10 mM, the diffraction was blue-shifted. This occurred because the crown ethers were saturated above 5 mM Pb^{2+} and further increases in Pb^{2+} concentration resulted in a decreased Donnan osmotic pressure at higher ionic strengths.[10] Figure 5c clearly shows the visually evident color changes that occur with changing pH values.

These 2-D photonic crystal sensors are capable of detecting extremely small quantities of analytes. For example, when we utilized a visually evident sensor with an area of 1 mm² attached to a 10 μm thick hydrogel layer, we could sense a sample volume of ∼10^{-5} mL. Figure 5a indicates a detection limit of much less than 0.1 mM Pb^{2+}. Thus, we can detect <10^{-12} mol of Pb^{2+}.

These 2-D arrays have multiple advantages over the previous 3-D photonic crystals. For example, the 2-D array hydrogel can be functionalized with molecular recognition agents prior to attachment of the 2-D array. In the case of the 3-D CCA, the functionalization chemistry must be homogeneous to avoid

disordering the 3-D array. In addition, we monitor only the 2-D array spacing on micrometer-thick films. Such thin films allow fast detection of small volumes because of rapid diffusion. It is not necessary to utilize self-assembled colloidal particle arrays; any 2-D array of sufficient refractive index modulation will work.

In summary, we have demonstrated ultrahigh-diffraction-efficiency 2-D particle array materials that can be utilized for chemical sensing. These hydrogel films can be tailored to detect many molecular analytes and biological agents. We expect that these 2-D photonic sensing materials will find applications in visual chemical detection.

■ ASSOCIATED CONTENT

Ⓢ Supporting Information.   PS particle synthesis, 2-D array preparation, sensing conditions, and a figure showing pH diffraction reversibilities. This material is available free of charge via the Internet at http://pubs.acs.org.

■ AUTHOR INFORMATION

Corresponding Author
asher@pitt.edu

■ ACKNOWLEDGMENT

■ REFERENCES

(1) (a) Cao, Q.; Rogers, J. A. *Adv. Mater.* **2009**, *21*, 29. (b) De, M.; Rana, S.; Akpinar, H.; Miranda, O. R.; Arvizo, R. R.; Bunz, U. H. F.; Rotello, V. M. *Nat. Chem.* **2009**, *1*, 461. (c) Lee, Y. J.; Braun, P. L. *Adv. Mater.* **2003**, *15*, 563. (d) Hendrickson, G. R.; Smith, M. H.; South, A. B.; Lyon, L. A. *Adv. Funct. Mater.* **2010**, *20*, 1697. (e) Shin, J.; Braun, P. V.; Lee, W. *Sens. Actuators, B* **2010**, *150*, 183.

(2) (a) Wang, J. *Chem. Rev.* **2008**, *108*, 814. (b) Borisov, S. M.; Wolfbeis, O. S. *Chem. Rev.* **2008**, *108*, 423. (c) LaFratta, C. N.; Walt, D. R. *Chem. Rev.* **2008**, *108*, 614.

(3) (a) Hu, X.; Huang, J.; Zhang, W.; Li, M.; Tao, C.; Li, G. *Adv. Mater.* **2008**, *20*, 4074. (b) Miyaji, H.; Sato, W.; Sessler, J. L. *Angew. Chem., Int. Ed.* **2000**, *39*, 1777. (c) Pu, K. Y.; Liu, B. *Adv. Funct. Mater.* **2009**, *19*, 1371.

(4) (a) Ben-Moshe, M.; Alexeev, V.; Asher, S. *Anal. Chem.* **2006**, *78*, 5149. (b) Walker, J.; Kimble, K.; Asher, S. A. *Anal. Bioanal. Chem.* **2007**, *389*, 2115. (c) Shi, L.; Virji, M.; Finegold, D.; Asher, S. A. *J. Am. Chem. Soc.* **2004**, *126*, 2971. (d) Huang, G.; Hu, Z. *Macromolecules* **2007**, *40*, 3749. (e) Xia, Y.; Gates, B.; Yin, Y.; Lu, Y. *Adv. Mater.* **2000**, *12*, 693. (f) Lawrence, J. R.; Shim, G. H.; Jiang, P.; Han, M. G.; Ying, Y.; Foulger, S. H. *Adv. Mater.* **2005**, *17*, 2344.

(5) (a) Lee, M.; Fauchet, P. M. *Opt. Express* **2007**, *15*, 4530. (b) Yu, X.; Shi, L.; Han, D.; Zi, J.; Braun, P. V. *Adv. Funct. Mater.* **2010**, *20*, 1910.

(6) Dimitrov, A. S.; Dushkin, C. D.; Yoshimura, H.; Nagayama, K. *Langmuir* **1994**, *10*, 432.

(7) Kanai, T.; Sawada, T.; Kitamura, K. *Langmuir* **2003**, *19*, 1984.

(8) Tikhonov, A.; Kornienko, N.; Zhang, J.; Asher, S. A. Submitted.

(9) Xu, X.; Goponenko, A. V.; Asher, S. A. *J. Am. Chem. Soc.* **2008**, *130*, 3113.

(10) Holtz, J. H.; Holtz, J. S.; Munro, C. H.; Asher, S. A. *Anal. Chem.* **1998**, *70*, 780.